Kidney International, Vol. 64 (2003), pp. 1253–1264

Altered mRNA expression in renal biopsy tissue from patients with IgA nephropathy

Iwao Waga, Jun Yamamoto, Hitoshi Sasai, William E. Munger, Susan L. Hogan, Gloria A. Preston, Hong-Wei Sun, J. Charles Jennette, Ronald J. Falk, and David A. Alcorta

JT Frontier Research Laboratories, Japan Tobacco, Inc., Yokohama, Kanagawa, Japan; Gene Logic, Inc., Gaithersburg, Maryland; Department of Pathology and Laboratory Medicine and Department of Medicine, Division of Nephrology and Hypertension, University of North Carolina at Chapel Hill, Chapel Hill, North Carolina

Altered mRNA expression in renal biopsy tissue from patients with IgA nephropathy.

Background. Immunoglobulin A (IgA) nephropathy (IgAN) is a renal disease characterized by glomerular deposition of IgA-dominant immune deposits that cause glomerular inflammation and sclerosis. Gene expression changes induced in renal tissues/cells as a result of the disease are largely uncharacterized.

Methods. A sensitive differential mRNA display technique, restriction endonucleolytic analysis of differentially expressed sequences (READS®) compared similarly processed normal renal tissue to renal biopsy RNA from patients with IgAN, minimal change disease, and necrotizing crescentic glomerulonephritis. A subset of genes with altered expression in IgAN as identified by the READS® technology was further characterized and expression levels confirmed using real-time quantitative polymerase chain reaction (RT-PCR) analysis (TaqMan®) in all RNA.

Results. Initial READS® analysis showed IgAN samples have lower mRNA levels relative to normal renal tissue mRNA samples based upon total RNA as measured by ribosomal RNA. One hundred seventy-five differentially expressed nonredundant fragments were found from 860 initial candidate fragments. Twenty genes were selected for additional TaqMan® analysis, and 13 of 20 genes showed statistically different expression when comparing biopsies from normal individuals and IgAN patients. Expression differences were seen in these genes in biopsies of IgAN of differing clinical activities. Gene expression cluster analysis using the Ward method detailed disease- and gene-related clusters. Detailed examination of the promoter regions of the genes within two gene clusters revealed common gene transcriptional regulatory protein-binding sites.

Conclusion. IgAN leads to significant changes in overall mRNA transcription levels within the renal tissue, in addition to gene-specific mRNA level changes. Disease-related patterns of expression were identified and gene-specific clusters suggest common mechanisms of transcriptional alteration.

Key words: gene expression, IgA nephropathy, differential display, renal biopsy, cluster analysis, mRNA.

Received for publication November 26, 2002
and in revised form April 18, 2003
Accepted for publication May 23, 2003

Immunoglobulin A (IgA) nephropathy (IgAN), first described by Berger and Hinglais in the mid-1960s [1], is characterized by significant deposition of IgA-rich immune complexes in the glomeruli of the kidney [2]. IgAN was initially believed to be uncommon and to have a relatively benign progression, but demographic and longitudinal studies have shown that IgAN is the most common glomerular disease in the world and is a significant cause of end-stage renal disease [3]. Mounting evidence suggests that IgAN may have a genetic predisposition with respect to its development and progression. There are clear ethnic differences in the occurrence of IgAN. Molecular analysis has shown an association with genetic polymorphisms in the angiotensin-converting enzyme (ACE), the angiotensin II receptor 1, the T-cell receptor, and specific major histocompatibility class II genes [4]. Recently, Ghavari et al [5] demonstrated an association using a linkage analysis to a gene(s) within chromosomal localization of 6q22-23 in familial IgAN. How or whether these genotypic features relate to the important pathogenetic abnormalities in IgA1 glycosylation remains unclear [6].

In this study, we used the technique of mRNA differential display to compare normal renal tissue to renal biopsy material from patient biopsies with IgAN, minimal change disease, and necrotizing crescentic glomerulonephritis (NCGN). Using mRNA differential display technology, we report here overall lower mRNA levels relative to the total RNA isolated and identify a subset of genes with altered expression in renal biopsy tissue from IgAN patients that were largely confirmed by quantitative reverse transcription-polymerase chain reaction (RT-PCR). Semi-quantitative renal disease activity scores for the IgAN patients were determined for the biopsy sample set and clustered with the gene expression levels of the selected gene subset using the Ward cluster method. Four clusters of patients primarily representing normal, mildly active IgAN, moderately/severely active IgAN,

and necrotizing crescentic glomerulonephritis biopsies were identified based upon similar gene expression patterns. Additionally, clustering delineated three distinct gene clusters, and bio-informatic analysis of promoter sequences of two genes from two of the gene clusters revealed several promoter elements in common for the genes within each cluster. The promoters in common with different classes of gene clusters suggest a mechanism for widespread change in gene expression and perhaps thereby modulating disease activity in IgAN.

METHODS

Biopsy material and RNA

Tissue was obtained from clinical renal biopsies collected at the University of North Carolina, Chapel Hill, under a UNC Internal Review Board–approved protocol. Renal tissue was mounted in O.C.T. compound (Tissue-Tek, Torrance, CA, USA) and stored at −70°C after processing for pathologic diagnosis. Tissue was removed from the OCT block by excision while frozen and processed to total RNA using Trizol reagent (Life Technology, Rockville, MD, USA). Tissue culture cells were isolated using RNAStat 60 (Teltest, Inc., Friendswood, TX, USA) following the manufacturer's protocol.

For gene expression analysis, IgAN specimens were compared to disease controls with minimal change disease (MCD), pauci-immune necrotizing crescentic glomerulonephritis (NCGN), and to normal control renal tissue. Normal renal tissue samples were obtained by needle biopsies of kidneys from traumatic death patients or from normal margins after resection of renal cell carcinomas, and frozen before processing to replicate sample conditions used for disease-related biopsies. Due to the small RNA yields from each biopsy and significant RNA amounts required for the differential display technique used in these studies, RNAs were pooled. Seven normal samples were divided into 3 pools, while single pools were made from the 4 MCD patients and 4 NCGN patients. For IgAN clinical subgroups, biopsies from 4 mild, 4 moderate, and 4 severe patients were pooled to give mild, moderate, and severe pooled sample groups. Clinical activity of the IgAN samples was determined by the simultaneous review of the patients' clinic notes, pathology reports of biopsy tissues, and renal function assessed by the serum creatinine and the degree of hematuria and proteinuria. Two members of our group (RJF and JCJ) used this information to classify IgAN into 4 groups of patients with mild, moderate, or severe disease and a group of patients in remission. Classification of degree of clinical disease activity was as follows: (*1*) mild disease activity was defined as the presence of hematuria with <1 g proteinuria with normal renal function; (*2*) moderate disease activity was defined as the presence of hematuria with >1 g proteinuria and stable renal function; and (*3*) severe disease activity was defined as progression to renal insufficiency with hematuria and >1 g of proteinuria. Patients were considered in remission if there was no evidence of hematuria, <1 g of proteinuria, and no evidence on renal biopsy of active glomerular inflammation (i.e., hypercellularity, necrosis, or cellular crescents). Tissue from 4 patients with MCD and 4 patients with pauci-immune necrotizing and crescentic glomerulonephritis served as disease controls. Realizing the fundamental bias caused by the pooling process we verified by quantitative RT-PCR the expression levels of genes of interest in a panel of additional biopsy RNA samples. This expanded patient biopsy RNA panel consisted of 42 biopsy samples with 10 normal, 7 minimal change, 6 mildly active IgAN, 7 moderately active IgAN, 4 severely active IgAN, and 8 NCGN, and included the RNA used for differential display analysis.

Human cultured primary cells [umbilical arterial endothelial (HUA), umbilical venous arterial (HUV), tubular epithelial (EPI), and mesangial cells (Mes)] were obtained from Clonetics (San Diego, CA, USA) and grown per the company's instructions. Growth arrest conditions were growth to saturation density by extended cultivation, or treatment with 2 ng/mL human recombinant tumor necrosis factor-α (Collaborative Research, San Diego, CA, USA) for specified times. Peripheral blood leukocytes were isolated following removal of red blood cells by hypotonic lysis as detailed previously [7].

mRNA expression analysis

Differential display expression analysis is a powerful technique to determine altered expression of a large number of genes between a limited number of sample RNAs. The method that we used is known as restriction endonucleolytic analysis of differentially expressed sequences (READS®). READS® is an enhanced differential display technology that visualizes nearly all mRNAs expressed in a given sample and allows the determination of the differentially expressed sequences between samples by visual or densitometric analysis [8]. cDNA from each pool was generated with each of 12 possible different heel primers using an adapter oligo-d(T) with the various combinations of A, C, G, or T resulting from substitutions at the last 2 base positions in each primer. Each cDNA from a sample mRNA/primer combination was digested independently with 8 different 6 base-recognition restriction enzymes (PstI, NcoI, SacI, XbaI, BsrGI, XhoI, HindIII, MunI). Following adapter ligation, PCR products were labeled during amplification using α-^{33}P-ATP for finer band resolution. Product bands were resolved by sequencing gel separation. This combination of primers and restriction enzymes resulted in approximately 80% of the expressed genes being visualized. Autoradiographs of the gels were scanned visually for expression differences and sequences of the differen-

tially expressed bands were determined by coring the gel, band elution, product amplification, and sequencing. The READS® processing and initial bioinformatics analysis was performed at Gene Logic, Inc. (Gaithersburg, MD, USA). The READS® method is a proprietary process covered by patents #6,010,850, #5,712,126, and #6,395,887.

Quantitative RT-PCR

Genes of interest identified by READS® were selected for more detailed analysis using quantitative RT-PCR. Primers and probes for TaqMan® analysis were designed using Primer Express 1.5 (Applied Biosystems, Foster City, CA, USA) using company guidelines from sequence information from GenBank or EST databases. For each gene, one-tenth to 1 ng of the individual biopsy total RNA was analyzed on an ABI PRISM 7700 using TaqMan® EZ RT-PCR Core Reagent kit (Applied Biosystems). All TaqMan® analysis was done using 3 primers PCR (forward and reverse primers with fluorescent probe) to ensure specificity of signal. Fold-change analysis was based on standardizing RNA levels by correcting for glyceraldehyde-3-phosphate dehydrogenase (GAPDH) levels in the sample.

Statistical analysis and data mining

Overall differences between multiple groups were tested using the non-parametric Kruskal-Wallis test and analysis of variance. When distributions were not normally distributed, ranked values were used for analysis of variance tests. Fold-change values for all genes except protein disulfide isomerase and EST23476 were not normally distributed so that ranked values were used for analysis of the other 18 genes. If there was an overall difference between groups using these tests ($P < 0.05$), then Duncan's multiple-range test was used to evaluate differences between specific group means, while controlling the error rate from multiple comparisons. Fold-change data determined by TaqMan® Q-RT-PCR analysis was subjected to cluster analysis using the Ward's method [9] based upon the squared Euclidean distance for each gene, in which the mean of the normal samples was set to 0. The calculated results are plotted in Figure 3. DNA sequence analysis of promoter regions was performed on sequences downloaded from GenBank using Omiga software (Accelrys, Princeton, NJ, USA) and the public web search site, TFBINF, for transcription factor binding sites (website no longer on-line) [10].

RESULTS

Initial analysis of READS® gels showed a significant difference in overall signal intensity between gels derived from normal renal tissue and from either the IgAN or NCGN pools (Fig. 1A). A representative gel shows the comparable signal intensity in normal samples in lanes 1 to 3, while IgAN with a range of clinical activities is shown in lanes 4 to 6, and NCGN, in lane 7, show significantly lower band intensities. RNA quantity and quality of the total RNA from all of the samples were similar (data not shown), thus eliminating RNA degradation as a cause for this difference. These results suggested lower levels of message present, while the predominant RNAs in total RNA, the 28S and 18S ribosomal RNAs (rRNA), were expressed at a constant level in all samples. To further explore this difference, quantitative RT-PCR levels of GADPH mRNAs in these samples were compared to 28S rRNA levels. The ratios of the average levels of GAPDH and 28S rRNA expression were calculated for the normal and IgAN samples. One healthy control biopsy sample was used as a standard and all other sample ratios were divided by this initial ratio; then, the average for each group was normalized to the normal sample average and the standard deviations corrected proportionally. The average and standard deviation of the normal and IgAN biopsies are shown in Figure 1B and revealed that the IgAN ratio was greater than 3-fold lower than the ratio of average GAPDH and 28S rRNA levels from the normal control biopsy RNAs. This decrease was a statistically significant, $P < 0.01$. Comparable results were seen when similar comparisons were done with mitochondrial DNA–dependent transcripts and 18S rRNA levels (data not shown). As different RNA polymerases transcribe rRNA and mRNAs, RNA polymerase I and II, respectively, we examined the expression level of another RNA polymerase II transcribed gene, γ-actin, and compared its level to GAPDH. This comparison shows whether the initial difference in the GAPDH/28S rRNA ratio is due to lower expression of GAPDH only, or, alternatively, if it is due to a systemic change in the RNA polymerase II transcribed RNA expression. The fact that a similar difference was seen with mitochondrial transcripts argues the rRNA levels were not abnormally elevated. Following similar averaging and ratio calculation as performed for GAPDH and 28S rRNA, we found no significant difference in GAPDH/γ-actin ratio for IgAN samples compared to normal individuals (Fig. 1C). This result shows that these two RNA polymerase II transcribed "housekeeping" messages are similarly expressed in IgAN and suggests the lower READS® gel intensity reflects a decrease in overall message synthesis in IgAN tissue samples. To overcome this difference, 4- to 8-fold larger amounts of product were loaded per lane, which equalized the overall gel intensity in normal and disease-derived samples and allowed the identification of differentially expressed messages (Fig. 1D).

Initial identification of expression differences was done by visual examination and 860 products were identified as potentially different between diseases and nor-

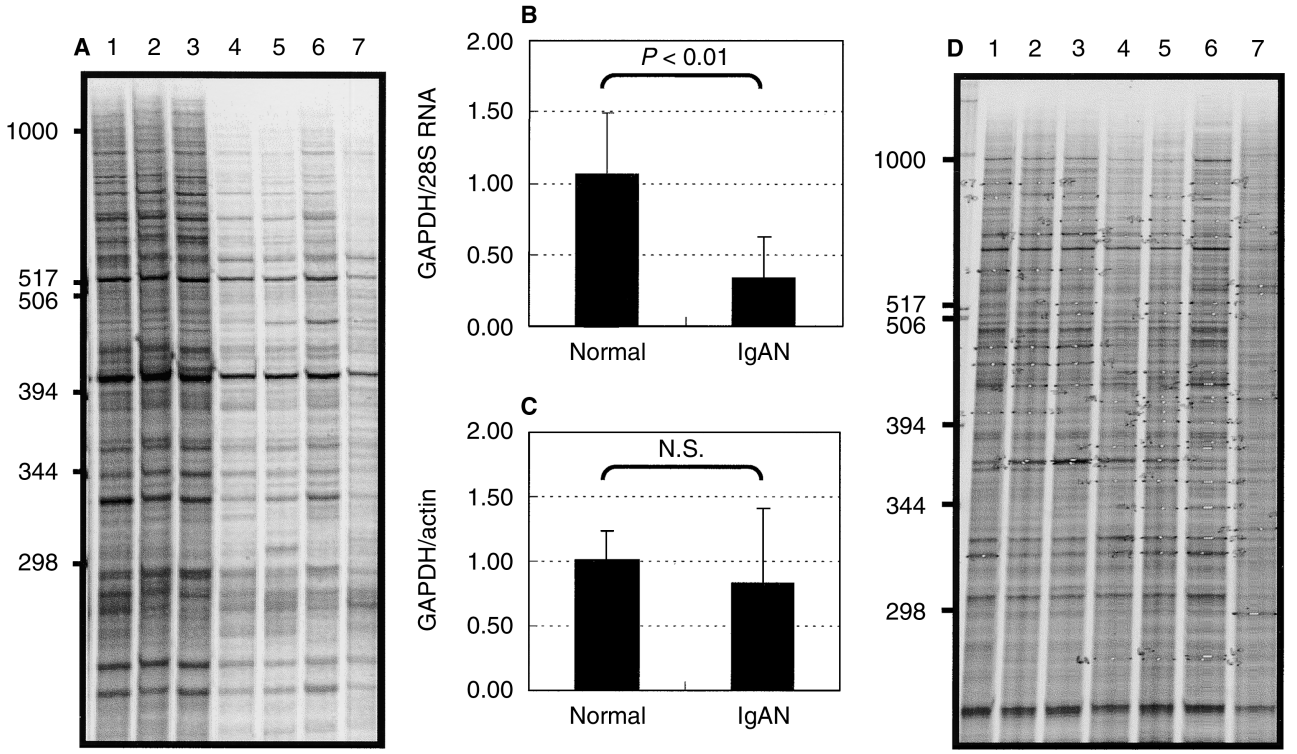

Fig. 1. Molecular analysis of pooled biopsy samples. (*A*) Representative restriction endonucleolytic analysis of differentially expressed sequences (READS®) gel showing analysis performed on normal tissue (lanes 1 to 3), immunoglobulin A nephropathy (IgAN) with clinical activity; mild (lane 4), moderate (lane 5), severe (lane 6), and necrotizing crescentic glomerulonephritis (NCGN) (lane 7), using standard loading criteria. Significantly lower message levels are seen in IgAN and NCGN samples. (*B*) An average of the ratio of the relative expression levels of GAPDH and 28S rRNA levels within the individual biopsy RNAs for normal and IgAN samples, as determined by quantitative real-time-polymerase chain reaction (RT-PCR). The average of the normal samples was set to one. A statistically significant decrease in the ratio of the IgAN samples shows decreased message levels. (*C*) Similar averages of the ratios as in B, but for GAPDH and γ-actin mRNAs show no difference in gene levels in normal versus IgAN samples. (*D*) READS® analysis on similar samples as in (A), with increased sample loading, shows comparable signal intensity. PCR cores for re-amplification and sequencing were removed from PCR products following overlaying and alignment of the autoradiograph and are seen as white spots in the middle of the autoradiographic bands.

mal samples, and for one or multiple clinical states for the IgAN samples. From these 860, 175 non-homologous messages were found based upon sequencing the re-amplified and sequenced PCR bands excised from the original gels (Fig. 1D). Examples of READS® gels representing potentially differentially expressed fragments are shown in Figure 2. Bands were removed, sequenced, and subsequently identified as expressed sequence tags (ESTs) 22402, 22972, and 22360. From the 175 sequences, 20 were selected for more detailed analysis by quantitative RT-PCR based upon the largest intensity differences, disease specific changes, and expression variation in samples of differing IgAN clinical activity (Table 1). This list of genes includes six ESTs and known genes, such as cathepsin D, napsin, TSC22, 45 kD megalin-binding protein (MBP45K), a putative protease inhibitor HE4, and the metalloprotease inhibitor TIMP1.

Statistical analysis of changes in gene expression was performed for protein disulfide isomerase (PDI) and EST23476 using untransformed fold-change values while the fold-change values for other 18 genes were not nor-

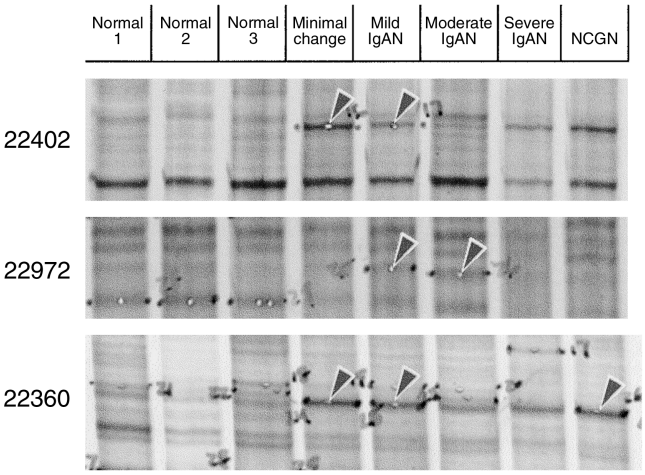

Fig. 2. Representative restriction endonucleolytic analysis of differentially expressed sequences (READS®) analysis of specific genes identified as altered in disease. Differentially expressed fragments are identified by arrowheads, and subsequently were identified by sequencing and denoted ESTs 22402, 22972, and 22360.

Table 1. Fold change data

Name	Abbreviation	Accession #	Healthy control vs. Minimal change	Healthy control vs. IgAN-all	Healthy control vs. NCGN	Other comparisons MC × IgA	Other comparisons MC × NCGN	Other comparisons IgA × NCGN	Healthy control vs. IgA clinical activity Mild	Healthy control vs. IgA clinical activity Moderate	Healthy control vs. IgA clinical activity Severe	Other comparisons Mild × mod	Other comparisons Mild × sev	Other comparisons Mod × sev
EST	22972	AA132448	1.31	2.90	2.01				2.42	4.40	1.15			S
Lipoprotein-related protein-associated protein 1[a]	MBP45k	NM_002337	2.68	3.19	1.89			S	3.16	4.04	1.85		S	S
NYCO-28	GN01	NM_006645	1.88	2.65	0.68		S	S	3.08	3.07	1.46			S
EST	22360	AA873801	2.83	3.02	0.53			S	2.56	4.85	0.89		S	S
Ubiquitin-protein ligase NEDD4-like	22402	AF070601	1.88	4.98	0.68	S	S	S	5.25	6.82	1.78		S	S
Lipoprotein receptor-related protein 2 precursor (megalin)	gp330	NM_004525	2.41	4.66	1.60			S	5.04	5.27	3.23			
Prolyl 4-hydroxylase alpha-2	Prolyl2	NM_004199	5.90	3.65	1.16		S	S	3.81	4.10	2.99		S	S
Epididymis-specific protein E4 precursor	22962 (HE4)	NM_006103	1.97	1.79	3.27				1.64	1.36	2.91			
Tissue inhibitor of metalloproteinases 1	TIMP1	NM_003254	2.11	1.52	3.33			S	1.39	1.79	1.38			
GA-binding protein binding transcription factor (GABPH)	E4TF1-47	NM_002041	1.89	2.21	1.65				2.39	2.47	1.71			
Cathepsin D	CathD	NM_001909	1.83	1.81	2.26				1.76	2.35	1.08			S
Human small zinc finger-like protein	Zinc29in4628 (Zinc29)	AF144700	1.44	1.81	1.04		S	S	1.85	2.03	1.45			
Protein disulfide isomerase[b]	PDI	NM_006849	1.39	1.99	1.44	S			1.71	2.36	1.84			
Prolyl 4-hydroxylase alpha-1	Prolyl1	NM_000917	1.34	1.45	1.16				1.52	1.46	1.16			
EST[b]	23476	THC219317	1.18	1.88	0.88			S	2.07	1.93	1.44			
TGF-β stimulated clone 2	TSC22	NM_006022	0.41	0.88	0.38			S	0.70	1.13	0.74			
Napsin, apartyl protease 4	Napsin	NM_004851	1.28	0.99	1.15				1.33	0.82	0.76			
EST	43719	NP_112188	1.83	2.82	0.81			S	2.80	3.52	2.00			
EST-novel	45396	NA	1.67	1.72	0.45				1.90	1.89	1.11			
Osteoblast specific factor 2	23907 (OSF2)	NM_006475	2.30	8.23	1.99	S		S	5.31	11.73	7.91			

Shaded values and comparisons marked by "S" are significant by non-parametric Kruskel-Wallis and analysis of variance. $P < 0.05$ with Duncan range test of multiple groups.

[a] 45 kD megalin-binding protein

[b] Values normally distributed. Statistics done on unranked fold change values while all other comparisons done with ranked values

mally distributed and ranked values were used. Seventeen of the 20 selected genes showed statistically significant differences in comparing across all disease and IgAN clinical activity groups. In comparisons of normal biopsy expression levels with other diseases, 13 genes were altered in IgAN, 7 in MCD, and 12 in NCGN, with all the disease samples showing elevated expression levels, while there were 3 genes different between MCD and IgAN, 4 between MCD and NCGN, and 12 between IgAN and NCGN (Table 1). Only prolyl 4-hydroxylase alpha 1, napsin, and EST45396 were not altered in any comparison (normal vs. disease, normal vs. IgAN of different clinical activity, or disease vs. disease). In normal versus disease comparisons, two additional genes, TSC22 and EST 23476, were not altered, while MBP45k and GA-binding transcription factor (GABP), were altered in both normal versus disease and normal versus IgAN clinical activity comparisons, and cathepsin D was altered in all but the normal versus IgAN severe activity comparisons.

The 13 genes elevated in IgAN relative to the normal controls were ESTs 22972, 22360, 22402, and 43719, MBP45K, NYCO28, low density lipoprotein receptor-related protein 2 (gp330, megalin), prolyl 4-hydroxylase alpha-2 (prolyl2), GABP, cathepsin D, zinc29in4628 (zinc29), protein disulfide isomerase (PDI), and osteoblast-specific factor 2 (OSF2). Seven genes were altered in minimal change biopsies and six altered in NCGN with MPB45K, TIMP1, GABP, and cathepsin D common to both groups, with gp330, prolyl2, and zinc29 additionally altered in MCD, and EST22972 and HE4 altered in NCGN. A few genes were selectively altered in a single disease: PDI, EST43719, and OSF2 were elevated in IgAN, and HE4 altered only in NCGN, while the remaining 12 genes from normal/disease comparisons were altered in multiple diseases. Comparisons between disease groups showed 3 significant changes between MCD and IgAN, 4 between MCD and NCGN, and 12 between IgAN and NCGN. Most of these changes reiterate the normal versus disease comparison and are the result of a lack of a significant change of that disease type relative to normal but altered expression of EST23476 (1.88- to 0.88-fold relative to normal) and TSC22 (0.88- to 0.38-fold relative to normal) in the IgAN-NCGN comparison was not seen with any other comparison. The functional significance of these unique changes is unknown.

In comparisons of the normal control to the IgAN biopsies of differing clinical activities, the genes showing significant changes in the group as a whole are most closely correlated with those with mild and moderate activity, as 12 of the 13 genes were altered in both groups. In biopsies of mild clinical activity, only OSF2 was not altered, and in moderate clinical activity biopsies, EST 43719 was not changed. Significantly fewer changes were seen in the severe activity biopsies with ESTs 22972, 22360, and 43719, GN01, prolyl2, and cathepsin D was no longer significantly altered and with lower fold changes. EST43719 elevated in IgANs of mild activity was the only gene selectively over-expressed in a single clinical activity group.

In an attempt to determine if any of these genes showed disease-specific patterns of expression, the expression levels of the 20 genes in each of the 42 biopsies were subjected to the Ward method of cluster analysis and the individual sample expression values plotted with the associated clustering trees (Fig. 3). This analysis was done regardless of the type of renal disease. When analyzed for disease-related similarities, four distinct clusters were identified, as shown by the trees on the right of the figure. Examination of the patient population within each cluster showed a predominant representation within each individual group of normal, NCGN, mild IgAN, or moderate/severe IgAN biopsies. The large "normal" cluster contained all but one of the control biopsy samples but additionally contained three NCGN (denoted ANCA), two MCD, and three IgAN samples, while the remaining IgAN and NCGN clusters were strongly represented by patient samples with the predominant disease type or clinical activity. It is of interest that the mild IgAN subgroup was more closely related to the normal samples, especially in the cluster II and III genes, and to NCGN than to the more severe IgAN samples.

Cluster analysis also identified distinct gene subgroups within the 20 genes examined based upon similar patterns of gene expression. Three primary gene clusters were revealed, with cluster I containing the genes GN01, prolyl2, gp330, MBP45K, and ESTs 22360, 22972, and 22402; cluster II containing the largest number of genes with HE4, TIMP1, PDI, napsin, TSC22, prolyl1, cathepsin D, E4tf1, zinc29in4628, and ESTs 45396, 23476, and 43719; and cluster III containing a single gene OSF2.

To determine if these clusters represented significantly different expression profiles, the expression levels of representative genes from each cluster were determined on an expanded mRNA sample set containing additional biopsies from each disease, isolated peripheral blood leukocytes (PBLs), and cultured primary human endothelial, epithelial, and mesangial cells. MBP45K and HE4 were examined as representatives of cluster I and II expression profiles, respectively, and OSF2 for cluster III. MBP45K expression was detected in all biopsy samples with elevated levels in MCD and IgAN samples (Fig. 4A). Very low comparable expression levels were found in all of the cultured cells but were higher in PBL mRNAs (columns 63 to 68, Fig. 4B). Representative of cluster II, HE4 expression was most elevated in patients with NCGN and in tubular epithelial cells (Fig. 4 C and D). The level of HE4 increased dramatically in the growth-arrested epithelial cells induced by contact inhibition (Fig. 4B, lanes 57 to 59). Cluster III, OSF2 expres-

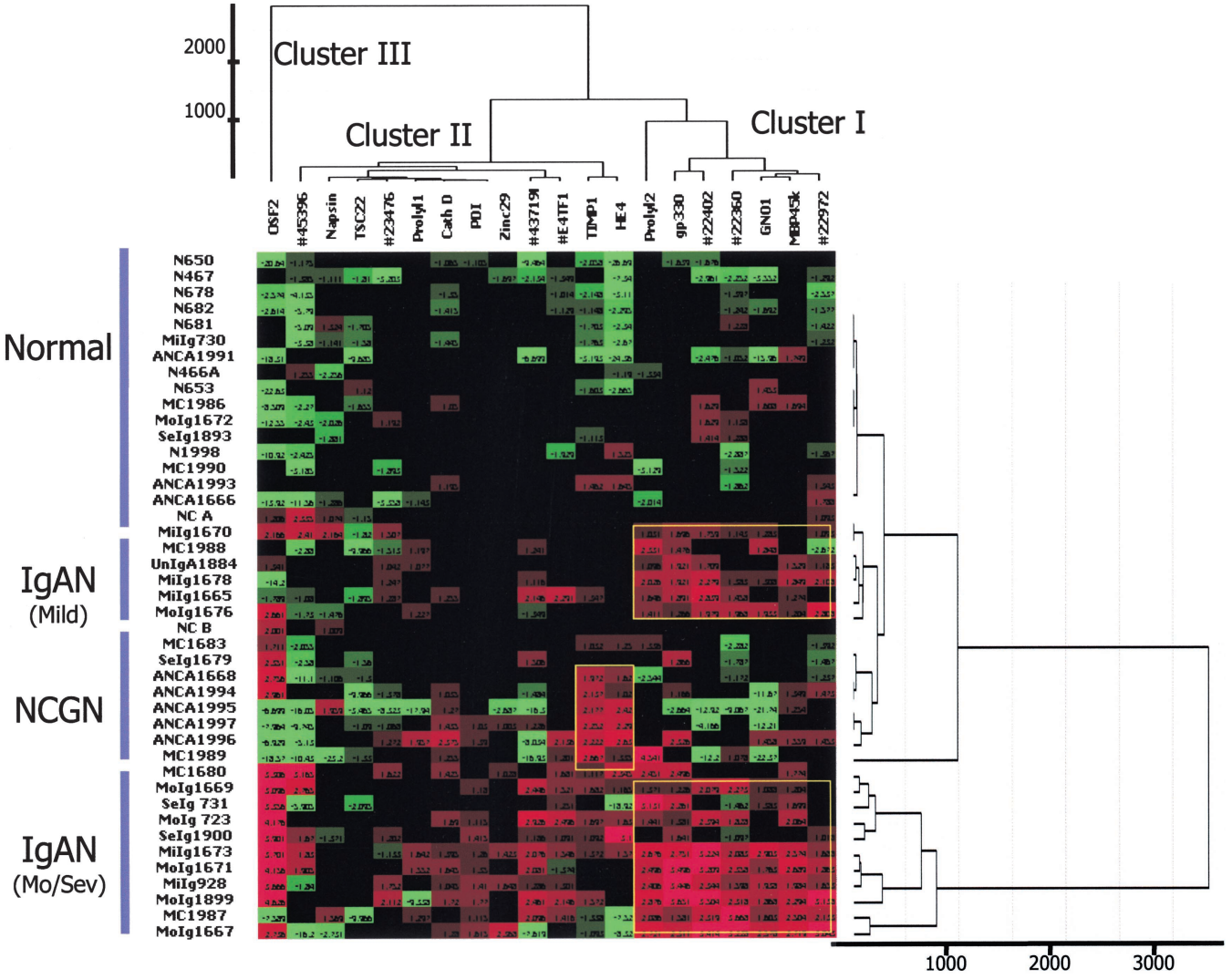

Fig. 3. Cluster analysis based on the expression levels of 20 representative restriction endonucleolytic analysis of differentially expressed sequences (READS®) genes in normal and diseased renal biopsy mRNAs. Relative expression levels were analyzed by the Ward method of clustering, based upon the squared Euclidean distance for each gene in which the mean of the normal control samples was set to 0. Individual sample levels are shown with elevated levels shown in increasing red color and lower levels shown in increasing intensities of green. Three gene clusters were found, while 4 patient clusters representing normal, predominantly clinically mild activity immunoglobulin A nephropathy (IgAN), anti-neutrophil cytoplasmic antibody (ANCA), and predominantly clinically moderate and severe IgAN. Individual samples were designated by the disease and sample number with N prefix used for normal, ANCA for necrotizing crescentic glomerulonephritis (NCGN), MCD for minimal change disease, and Mi, Mo-, Sev, or Un- with Ig used for mild, moderate, severe, or of unknown clinical activity for IgAN of different clinical activities.

sion was predominantly elevated in IgAN and arterial endothelial cells (Fig. 4 E and F). While the expression patterns in the biopsy RNAs were varied, their distinct expression patterns in the PBLs and cultured cells samples clearly distinguishes these genes and affirms the distinct clustering of the Ward method. Linear regression analysis using two cluster I genes, MBP45K versus gp330, and two cluster II genes, HE4 versus TIMP1, produced R^2 values of 0.48 and 0.69, respectively, showing the coordinate expression of each cluster's gene partners and reaffirming the cluster analysis. Regression analyis of cluster I with cluster II genes showed poor correlation values (data not shown).

Changes in messenger RNA expression levels are accomplished through a combination of both the regulation of transcription and modulation of message stability. Transcriptional activity is regulated through availability and/or activity of specific transcription factors. Thus, based upon the correlation of expression levels of the cluster genes detailed above, we examined upstream gene sequences of cluster I genes HE4 and TIMP1, and cluster II genes gp330 and MBP45K, to determine if these genes had common known or cryptic transcriptional regulatory elements in the promoter regions. The genomic sequences were analyzed and compared using bioinformatic tools. Binding sites for many transcription

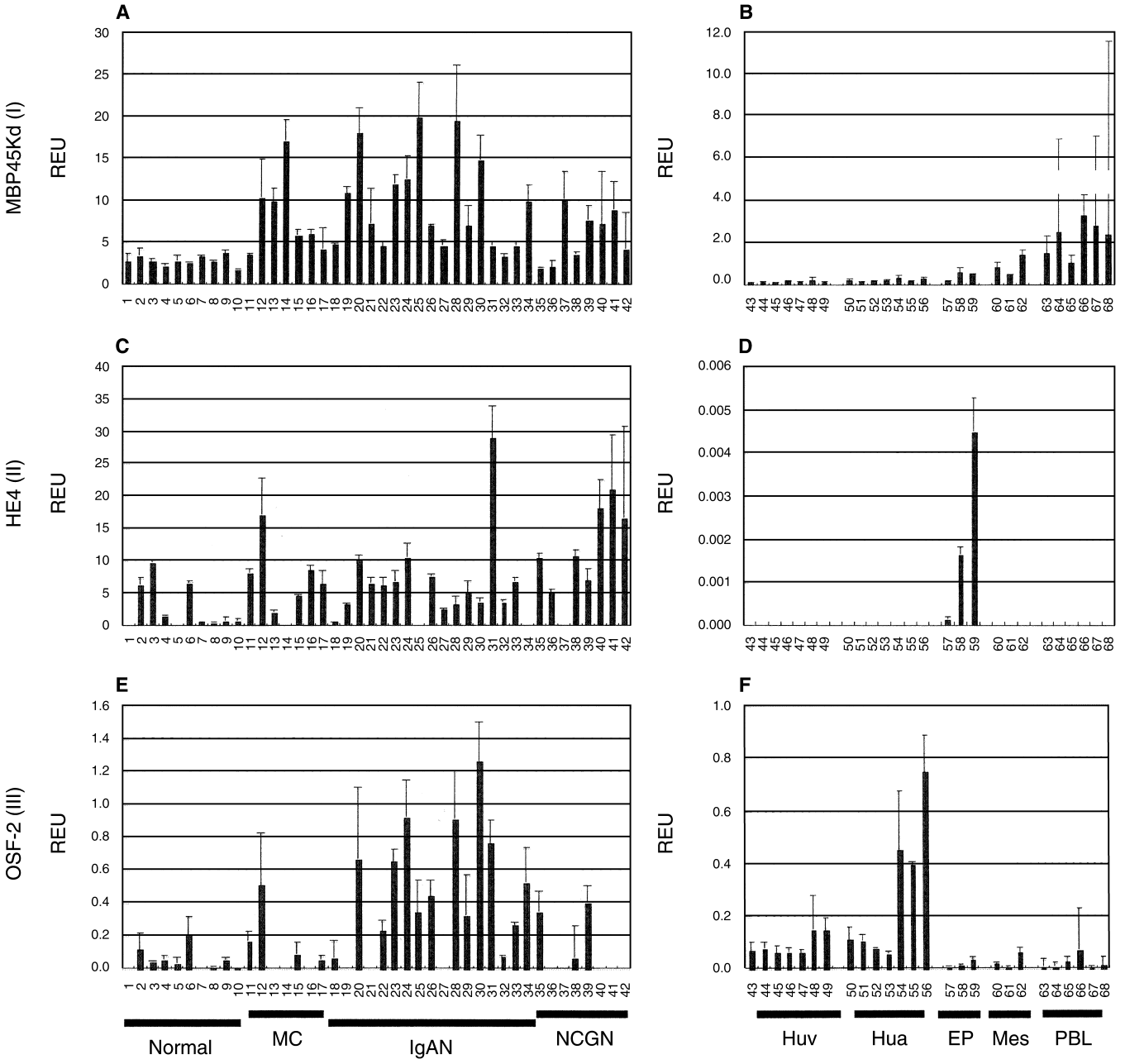

Fig. 4. mRNA expression levels of cluster I, II, and III genes in renal biopsies and cultured renal cells. Renal patient RNAs from normal, minimal change disease (MC), immunoglobulin A nephropathy (IgAN), and necrotizing-crescentic glomerulonephritis (NCGN) patients are shown in (*A*, *C*, and *E*), while expression profiles in primary human umbilical cord venous endothelial cells (Huv), human umbilical cord arterial endothelial cells (Hua), human renal epithelial cells (EP), human mesangial cells (Mes), and isolated peripheral blood leukocytes (PBLs) are seen in (*B*, *D*, and *F*). Expression of 45 kD megalin-binding protein (MBP45K) represented cluster I (A and C), HE4 represented cluster II genes (B and D), and OSF2 was the only member of cluster III (C and F). Renal patient RNAs for normal (lanes 1 to 10), MC (lanes 11 to 17), IgAN (mild activity, lanes 18 to 23, moderate clinical activity, lanes 24 to 30, and severe activity, lanes 31 to 34), and NCGN (lanes 35 to 42) are shown in (A, C, and E), while expression profiles in Huvs (lanes 43 to 49), Hua (lanes 50 to 56), EP (lanes 57 to 59), Mes (lanes 60 to 62), and PBLs (normal donors, lanes 63 and 64; IgAN patients, lanes 65 to 67, and one NCGN patient, lane 68). For Huv and Hua, cells were actively growing, treated with tumor necrosis factor-α for 1, 8, and 24 hours, or allowed to continue growing for 1, 4, and 5 days (saturation density), and are presented in that order. For Epi, cells were actively growing, or after 3 and 5 days growth to confluence and growth arrest while the Mes cells were actively growing or after 3 and 5 days growth to confluence and growth arrest.

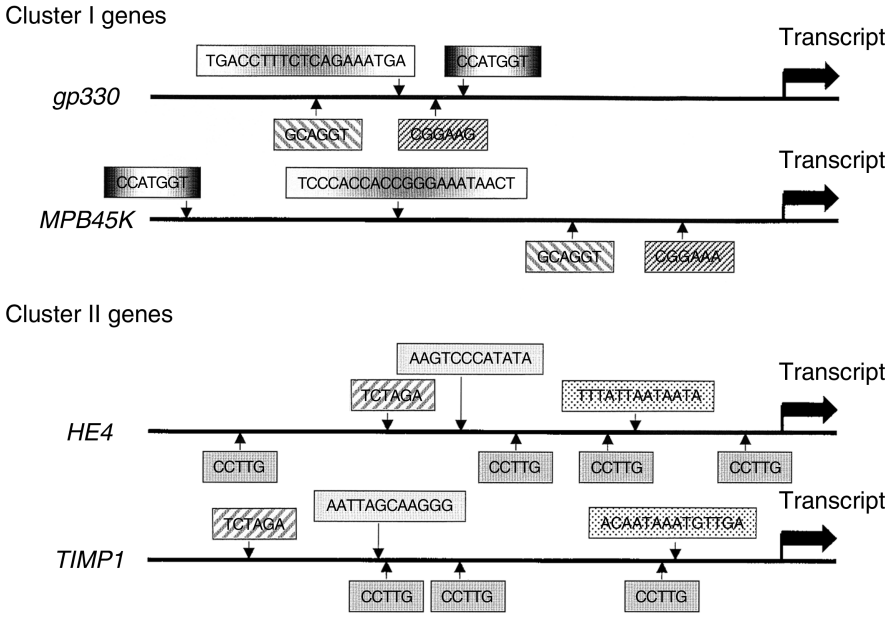

Fig. 5. Promoter regions of cluster I and cluster II genes. Genomic sequences of cluster I gp330 and MBP45K genes and cluster II HE4 and TIMP1 were analyzed for putative transcription factor binding sites. Upstream sequences of the putative promoter regions genes are shown (see Table 2 for description).

factors were found (Fig. 5 and Table 2). Of note, the GABP and Stat3 binding sites were found in cluster I genes, while MEF2, Oct1, XFD2, and many PBX1 binding sites were found in both cluster II genes HE4 and TIMP1. E4Tf1 transcription factor, elevated in the mild and moderate clinically active IgAN samples, binds to the GABP transcriptional site, suggesting a potential mechanism of altered gene expression.

DISCUSSION

Understanding the gene expression changes that occur within an affected tissue during the development and progression of a disease is the goal of current research, but given sample amount requirements for analysis with current technologies, few diseases and tissues have been reasonable targets for such detailed studies. Cancer is an exception and the molecular characterizations of mRNA expression patterns using high-density gene chip arrays of different breast cancers, lymphomas, and myelomas have dissected and differentiated disease subtypes and stages [11, 12]. These types of studies are the current paradigm for molecular genetics. Due to the difficulty of tissue access and abundance, dissection of renal disease has focused on the examination of in situ expression of single genes such as vascular permeability factor [13], C5a, [14], decay accelerating factor [15], and nitric oxide synthase [16], using cumbersome technology such as in situ mRNA hybridization.

We report here an examination of the mRNA expression profiles using mRNA differential display technology [8] of renal biopsy tissue from patients with MCD, IgAN, and NCGN. Dramatic expression changes were revealed in scope and specificity. Initial observations revealed a 70 to 85% reduction in the overall message levels in IgAN samples when compared to such standardization genes as mitochondrial DNA-dependent transcripts, or 18S and 28S rRNAs. But levels of both glyceraldehydes-3-phosphatase dehydrogenase (GAPDH) and γ-actin mRNAs were expressed at comparable levels in both normal or IgAN biopsies. GAPDH and γ-actin are transcribed by RNA polymerase II, while the rRNAs are transcribed by RNA polymerase I. Thus, a possible mechanism for such general expression differences may be explained by differences in RNA polymerase I and RNA polymerase II activities.

From the 175 potential candidate genes in the initial analysis using the differential display technique of READS®, the majority of these genes were elevated in disease. Of the 20 genes identified for further study, one gene elevated in IgAN biopsy samples is EST 22402, which has been identified as a human homolog of the yeast Rsp5 gene. Rsp5 is an ubiquitin ligase for RNA polymerase II [17]. Our working hypothesis is that up-regulation in IgAN renal tissue of EST 22402 could modulate the ubiquitination of RNA polymerase II and lead to decreased protein levels, which could ultimately result in the decreased message levels seen here. Additionally, of the 13 genes up-regulated in IgAN, changes in the 45 kD protein megalin-binding protein (MBP45K) and gp330 levels may have direct metabolic consequences due to the reported roles of gp330. The gp330 is the protein identified as the Heyman nephritis antigen [18] and is the multifunctional clearance receptor/low-density lipoprotein receptor–related protein 2 precursor (megalin) (glycoprotein 330), which binds to clusterin with high

Table 2. Position and frequency of known transcription factor binding sites in the cluster I gp330 and MPB45K genes and cluster II HE4 and TIMP1 genes

Promotor region and sequence		Class I				Class II			
		GP330		45 kD		HE4		TIMP1	
Name	Consensus sequence	Position	Hit site	Position	Hit site	Position	Hit site	Position	Hit site
GABP	CGGAAR	−1174	CGGAAG	−355	CGGAAA		ND		ND
Kozak	CCATGGT	−1071	CCATGGT	−1924	CCATGGT		ND		ND
AluTHEtarget	KCARGT	−1530	GCAGGT	−700	GCAGGT		ND		ND
rRNAspacer	TCTAGA		ND		ND	−1331	TCTAGA	−1722	TCTAGA
THEtarget	CCTTG		ND		ND	−1756	CCTTG	−1240	CCTTG
			ND		ND	−812	CCTTG	−1057	CCTTG
			ND		ND	−645	CCTTG	−422	CCTTG
			ND		ND	−227	CCTTG		ND
PBX1	ANCAATCAW		ND		ND	−1953	TTAAATGAT	−1143	ATTATTATT
			ND		ND	−1170	ACCTATCAT	−1140	ATTATTATT
			ND		ND	−511	TTGTTTATT	−1137	ATTATTGAT
			ND		ND	−508	TTTATTAAT	−944	ATCATTCAT
			ND		ND	−505	ATTAATAAT		ND
MEF2	CTCTAAAAATAACYCY		ND		ND	−785	AACCTTATTTGTACAG	−1107	TGTTAATCAGAACCCC
			ND		ND	−697	TGATAACAGTAACTCC		ND
XFD2	WNWATAAACAWNNR		ND		ND	−508	TTTATTAATAATAA	−385	ACAATAAATGTTGA
Oct1	TNTATGNTAATT		ND		ND	−1054	AAGTCCCATATA	−1245	AATTAGCAAGGG
STAT3	NGNNATTTCCSGGAA RTGNNN	−1315	TGACCTTTCTCAGAA ATGATA	−1301	TCCCACCACCGGGA AATAACT		ND		ND
		−83	GGGCTGTCCACGGA AATGCCA		ND		ND		ND

Sequences not found are denoted ND.

affinity [19]. Elevation of gp330 could lower the tissue or serum levels of clusterin, a condition that has been associated with nephritic syndrome in renal disease [20]. Additionally, this molecule has been identified as a potential drug receptor [21], as well as having the capacity to bind and uptake molecules such as plasminogen, extracellular matrix components, plasminogen activator-plasminogen activator inhibitor type I complex, apolipoprotein-e enriched beta-vldl, lipoprotein lipase, lactoferrin, and calcium [22–25]. Furthermore, gp330 has been shown in vitro to interact with thryoglobulin (tg) and mediate transcytosis of the gp330 and tg complex through thyrocytes, thus blocking the induction of the thyroid hormone T3, which is induced by tg endocytosis [26]. Modulation of gp330 levels has the potential to change the functional activity of a wide range of proteins linked to key metabolic processes that may contribute to the development of IgAN.

In NCGN, alteration of the protease/protease inhibitor balance may be involved in the pathologic process as elevated levels of the protease inhibitor TIMP1, the putative protease inhibitor HE4, and the protease cathepsin D were found in these biopsy RNAs. The aberrant activation of circulating neutrophils has been implicated in NCGN [27], and modulation of the granule protease by either heightened protease activity by addition of cathepsin D or by suppression of the protease activity by addition of inhibitors could be involved in the disease progression.

Another observation was that cluster analysis of the quantitative RT-PCR derived gene expression data delineated disease as well as gene specific clusters. Clustering by clinical diagnosis defined three clusters of samples representing predominantly biopsy samples from normal controls, NCGN, and two IgANs showing a predominance of either mild or moderate/severe disease activities. Only MCD samples did not show a distinct patient cluster. This lack of minimal change patient clustering is intellectually interesting but of unknown significance. Furthermore, this cluster analysis also revealed specific clusters of genes based upon related changes in the gene expression patterns in the panel of biopsy RNAs. As the genes in these clusters showed similar patterns of gene regulation, a more detailed bioinformatic analysis of several members of two classes revealed putative transcription factor binding sites common among genes of the same class. Specifically, GABP and Stat3 sites were found in cluster I genes, g330 and MBP45K, and MEF2, Oct1, and GABX consensus binding-site sequences were seen in cluster II genes HE4 and TIMP1. GABP with Stat3 is necessary for transcription of genes activated in the inflammatory process, such as interleukin-6 (IL-6). Changes in expression of genes regulated by GABP, in combination with an elevation of the transcription factor E4TF1-47 reported here, which binds to the GABP site (CGGAAR) [28], could account for the transcriptional changes and altered mRNA levels shown in IgAN. While the potential of these genes in changing leukocyte mRNA expression is apparent, additional studies of the genes in other clusters is needed to determine what role they have in the disease related changes in leukocyte metabolism.

CONCLUSION

We report the large-scale analysis of mRNA expression patterns in renal biopsy tissues from patients with minimal change disease, IgAN, and NCGN, and have confirmed by quantitative RT-PCR statistically significant changes in 17 of the original 20 READS® analysis-selected genes between all groups with 13 of these 17 altered between normal and IgAN samples. Characterization of the genes and clusters of genes with potentially common regulatory processes may allow one to begin dissecting the disease process occurring within the kidney. The ultimate goal is to identify those gene expression changes directly involved in initiation and/or pathogenesis and intervene with treatments at the appropriate times to return altered gene expression to normal levels [29]. While these studies have focused upon specific changes in kidney tissue, recent studies on lupus have characterized peripheral blood mononuclear cell expression profiles [30], and Mishra et al [31] have shown that in vitro treatment of lupus T-cells with a histone deacetylation inhibitor, trichostatin A, resulted in normalized levels of two over-expressed genes, interleukin-10 and cell-surface ligand CD40 (CD154), and an under-expressed gene, interferon-γ. It should be noted that trichostatin A induced a wide range of gene expression changes, but the effects on CD154, interleukin 10, and interferon-γ hint that the overall approach may be viable. Finally, we suggest that through the use of techniques such as differential display and high-density gene chip arrays on affected tissue(s), more detailed molecular analyses will point to individual genes and/or gene groups/clusters responsible for in situ pathologic processes, and ultimately leading to targeting these genes or modulation of their mRNA expression for therapy.

ACKNOWLEDGMENTS

The authors would like to thank Hyunsook Chin for assistance with the statistical analysis and Dr. Mike Kuziora of Gene Logic for our use of his Microsoft Excel program macro during data processing and graphing visualization for the cluster analysis results.

Reprint requests to Dr. David Alcorta, CB #7155, 315 MacNider Bldg., University of North Carolina, Chapel Hill, Chapel Hill, NC 27599-7155.
E-mail: dalcorta@med.unc.edu

REFERENCES

1. Berger J, Hinglais N: Intercapillary deposits of IgA-IgG. *J Urol Nephrol (Paris)* 74:694–695, 1968

2. Berger J: IgA glomerular deposits in renal disease. *Transplant Proc* 1:939–944, 1969
3. D'Amico G: The commonest glomerulonephritis in the world: IgA nephropathy. *Q J Med* 64:709–727, 1987
4. Hsu SI, Ramirez SB, Winn MP, *et al*: Evidence for genetic factors in the development and progression of IgA nephropathy. *Kidney Int* 57:1818–1835, 2000
5. Gharavi AG, Yan Y, Scolari F, *et al*: IgA nephropathy, the most common cause of glomerulonephritis, is linked to 6q22–23. *Nat Genet* 26:354–357, 2000
6. Amore A, Cirina P, Conti G, *et al*: Glycosylation of circulating IgA in patients with IgA nephropathy modulates proliferation and apoptosis of mesangial cells. *J Am Soc Nephrol* 12:1862–1871, 2001
7. Yang JJ, Preston GA, Pendergraft WF, *et al*: Internalization of proteinase 3 is concomitant with endothelial cell apoptosis and internalization of myeloperoxidase with generation of intracellular oxidants. *Am J Pathol* 158:581–592, 2001
8. Prashar Y, Weissman SM: READS: A method for display of 3′-end fragments of restriction enzyme-digested cDNAs for analysis of differential gene. *Methods Enzymol* 303:258–272, 1999
9. Ward JH: Hierarchical grouping to optimize an objective function. *J Am Stat Ass* 58:236–244, 1963
10. Tsunoda T, Takagi T: Estimating transcription factor bindability on DNA. *Bioinformatics* 15:622–630, 1999
11. Alizadeh AA, Staudt LM: Genomic-scale gene expression profiling of normal and malignant immune cells. *Curr Opin Immunol* 12:219–225, 2000
12. Perou CM, Sorlie T, Eisen MB, *et al*: Molecular portraits of human breast tumours. *Nature* 406:747–752, 2000
13. Brown LF, Berse B, Tognazzi K, *et al*: Vascular permeability factor mRNA and protein expression in human kidney. *Kidney Int* 42:1457–1461, 1992
14. Abe K, Miyazaki M, Koji T, *et al*: Enhanced expression of complement C5a receptor mRNA in human diseased kidney assessed by in situ hybridization. *Kidney Int* 60:137–146, 2001
15. Abe K, Miyazaki M, Koji T, *et al*: Expression of decay accelerating factor mRNA and complement C3 mRNA in human diseased kidney. *Kidney Int* 54:120–130, 1998
16. Hwang SM, Wilson PD, Laskin JD, *et al*: Age and development-related changes in osteopontin and nitric oxide synthase mRNA levels in human kidney proximal tubule epithelial cells: Contrasting responses to hypoxia and reoxygenation. *J Cell Physiol* 160:61–68, 1994
17. Beaudenon SL, Huacani MR, Wang G, *et al*: Rsp5 ubiquitin-protein ligase mediates DNA damage-induced the large subunit of RNA polymerase II in Saccharomyces. *Mol Cell Biol* 19:6972–6979, 1999
18. Farquhar MG, Saito A, Kerjaschki D, *et al*: The Heymann nephritis antigenic complex: Megalin (gp330) and RAP. *J Am Soc Nephrol* 6:35–47, 1995
19. Lemansky P, Brix K, Herzog V: Subcellular distribution, secretion, and posttranslational modifications of clusterin in thyrocytes. *Exp Cell Res* 251:147–155, 1999
20. Ghiggeri GM, Bruschi M, Candiano G, *et al*: Depletion of clusterin in renal diseases causing nephrotic syndrome. *Kidney Int* 62:2184–2194, 2002
21. Farquhar MG: The unfolding story of megalin (gp330): Now recognized as a drug receptor. *J Clin Invest* 96:1184, 1995
22. Lundgren S, Carling T, Hjalm G, *et al*: Tissue distribution of human gp330/megalin, a putative Ca(2+)-sensing protein. *J Histochem Cytochem* 45:383–392, 1997
23. Niemeier A, Willnow T, Dieplinger H, *et al*: Identification of megalin/gp330 as a receptor for lipoprotein(a) in vitro. *Arterioscler Thromb Vasc Biol* 19:552–561, 1999
24. Stefansson S, Lawrence DA, Argraves WS: Plasminogen activator inhibitor-1 and vitronectin promote the cellular clearance of thrombin by low density lipoprotein receptor-related proteins 1 and 2. *J Biol Chem* 271:8215–8220, 1996
25. Zlokovic BV, Martel CL, Matsubara E, *et al*: Glycoprotein 330/megalin: Probable role in receptor-mediated transport of apolipoprotein J alone and in a complex with Alzheimer disease amyloid beta at the blood-brain and blood-cerebrospinal fluid barriers. *Proc Natl Acad Sci USA* 93:4229–4234, 1996
26. Marino M, Zheng G, Chiovato L, *et al*: Role of megalin (gp330) in transcytosis of thyroglobulin by thyroid cells. A novel function in the control of thyroid hormone release. *J Biol Chem* 275:7125–7137, 2000
27. Preston GA, Falk RJ: ANCA signaling: Not just a matter of respiratory burst. *Kidney Int* 59:1981–1982, 2001
28. Watanabe H, Sawada J, Yano K, *et al*: cDNA cloning of transcription factor E4TF1 subunits with Ets and notch motifs. *Mol Cell Biol* 13:1385–1391, 1993
29. Alcorta DA, Prakash K, Waga I, *et al*: Future molecular approaches to the diagnosis and treatment of glomerular disease. *Semin Nephrol* 20:20–31, 2000
30. Maas K, Chan S, Parker J, *et al*: Cutting edge: Molecular portrait of human autoimmune disease. *J Immunol* 169:5–9, 2002
31. Mishra N, Brown DR, Olorenshaw IM, *et al*: Trichostatin A reverses skewed expression of CD154, interleukin-10, and interferon-gamma gene and protein expression in lupus T cells. *Proc Natl Acad Sci USA* 98:2628–2633, 2001